

# Background Semantics Matter: Cross-Task Feature Exchange Network for Clustered Infrared Small Target Detection With Sky-Annotated Dataset

Yimian Dai, Mengxuan Xiao, Yiming Zhu, Huan Wang, Kehua Guo, Jian Yang

**Abstract**—Infrared small target detection poses unique challenges due to the scarcity of intrinsic target features and the abundance of similar background distractors. We argue that background semantics play a pivotal role in distinguishing visually similar objects for this task. To address this, we introduce a new task—clustered infrared small target detection, and present DenseSIRST, a novel benchmark dataset that provides per-pixel semantic annotations for background regions, enabling the transition from sparse to dense target detection. Leveraging this dataset, we propose the Background-Aware Feature Exchange Network (BAFE-Net), which transforms the detection paradigm from a single task focused on the foreground to a multi-task architecture that jointly performs target detection and background semantic segmentation. BAFE-Net introduces a cross-task feature hard-exchange mechanism to embed target and background semantics between the two tasks. Furthermore, we propose the Background-Aware Gaussian Copy-Paste (BAG-CP) method, which selectively pastes small targets into sky regions during training, avoiding the creation of false alarm targets in complex non-sky backgrounds. Extensive experiments validate the effectiveness of BAG-CP and BAFE-Net in improving target detection accuracy while reducing false alarms. The DenseSIRST dataset, code, and trained models are available at <https://github.com/GrokCV/BAFE-Net>.

**Index Terms**—Infrared Small Target Detection; Clustered Target Detection; Dataset; Feature Exchange; Semantic Segmentation

## I. INTRODUCTION

INFRARED imaging has emerged as a crucial tool in various domains, particularly in scenarios where long-distance imaging is required in the absence of visible light, such as night-time operations or environments with limited visibility [1]. By capturing the thermal distribution of objects, infrared imaging provides critical information for applications such as unmanned system monitoring [2], maritime target search [3], and rescue missions [4]. However, in these applications, the targets of interest are often located at great distances, resulting in their appearance as extremely small-sized objects in the

captured images. Consequently, infrared small target detection plays a pivotal role in accurately interpreting and extracting valuable insights from these images, enabling the development of robust and efficient systems that can operate effectively in challenging conditions.

### A. Prior Works on Clustered Infrared Small Target Detection

While the potential of infrared imaging has been recognized across various domains, existing infrared small target detection techniques are predominantly tailored for the detection of sparse targets [5, 6], which proves to be inadequate when faced with complex application scenarios such as drone swarm defense, multi-target tracking systems, and extensive maritime search and rescue operations. Consequently, there is an urgent need for advanced technology capable of effectively identifying and tracking *dense infrared small targets*.

As the distribution of small targets transitions from sparse to dense scenarios, existing infrared small target detection techniques face a multitude of challenges that drastically hinder their effectiveness. *Firstly*, methods that rely on the assumption of sparsely distributed targets become inapplicable in dense scenes, where targets are closely situated and may occlude one another, leading to the breakdown of single-target analysis strategies. *Moreover*, the reliance on local contrast features [7, 8], a staple of traditional approaches, becomes unreliable as the targets are no longer set against a uniform background but are instead interspersed with other proximate objects. *Furthermore*, even state-of-the-art deep learning methods [9–12] struggle when confronted with dense target scenarios where the delineation between targets and background blurs, significantly adding to the complexity of detection tasks. Therefore, current methods are plagued by inefficiencies when operating in dense settings, frequently resulting in missed detections and high false alarm rates. This calls for new solutions tailored to overcome the intricacies of dense infrared small target detection.

From another perspective, despite the rapid strides made in generic object detection, with state-of-the-art methods like TOOD [13] and CrossKD [14] addressing dense object detection, these techniques cannot be directly transplanted to the domain of infrared small target detection. The challenges we face in this specialized field stem from several critical factors:

- 1) **Scarcity of Intrinsic Target Features:** The foremost challenge stems from the paucity of intrinsic target

This work was supported by the National Natural Science Foundation of China (62301261, 62361166670), the Fellowship of China Postdoctoral Science Foundation (No. 2021M701727). *The first two authors contributed equally to this work. (Corresponding author: Yiming Zhu and Huan Wang).*

Yimian Dai, Mengxuan Xiao, Yiming Zhu, Huan Wang, and Jian Yang are with School of Computer Science and Engineering, Nanjing University of Science and Technology, Nanjing, China. Yimian Dai and Jian Yang are also with PCALab, Key Lab of Intelligent Perception and Systems for High-Dimensional Information of Ministry of Education, and Jiangsu Key Lab of Image and Video Understanding for Social Security. (e-mail: [yimian.dai@gmail.com](mailto:yimian.dai@gmail.com); [yiming\\_zhu\\_grokc@163.com](mailto:yiming_zhu_grokc@163.com); [wanghuan-phd@njust.edu.cn](mailto:wanghuan-phd@njust.edu.cn); [csjyang@mail.njust.edu.cn](mailto:csjyang@mail.njust.edu.cn)).

Kehua Guo is affiliated with School of Computer Science and Engineering, Central South University, Changsha 410083, China. (e-mail: [guoke-hua@csu.edu.cn](mailto:guoke-hua@csu.edu.cn)).

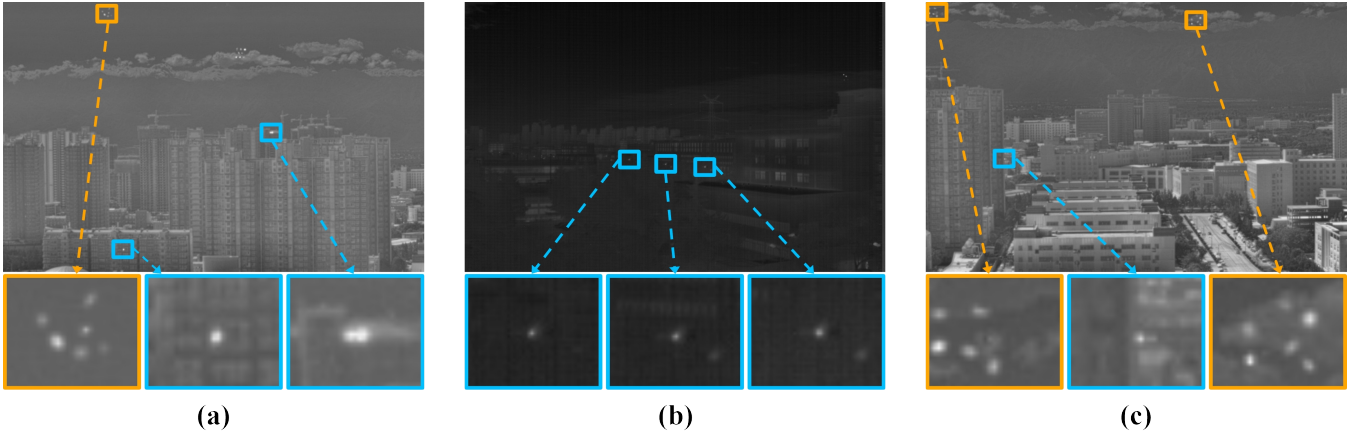


Fig. 1. The small target in the orange box is the real object we are interested in in the sky background, and the small target in the blue box is a virtual alarm in the background of the building. Figure (a) and Figure (c) show clustered small targets against the background of the sky and false alarms against the background of buildings, and figure (b) shows false alarms against the background of buildings.

features. Unlike generic objects, which boast rich visual cues such as appearance, texture, and structure, infrared small targets are minuscule in size, merely popping out as nondescript blobs in the image. This “visual poverty” renders recognition and localization methods based on target-specific characteristics largely ineffectual.

- 2) **Abundance of Similar Background Distractors:** Infrared imagery is often plagued by a multitude of background distractors that bear a striking resemblance to the targets of interest. These distractors, such as noise spots and hot spots, also manifest as blobs, making it nearly impossible to discriminate between them and genuine targets based on local visual comparisons.

These challenges inevitably lead us to ponder a fundamental question: *What truly distinguishes visually similar objects in single-frame infrared small target detection, assigning them different class labels?* Unraveling this enigma holds the key to developing effective and robust algorithms for infrared small target detection, enabling them to navigate the unique challenges posed by this task.

### B. Motivation

In this paper, we posit that the answer to the aforementioned question lies in the *background semantics*. As illustrated in Fig. 1, visually similar small objects at a distance can be classified differently based on their surrounding context. A small object in the sky background is likely to be a target of interest, while the same object against a building backdrop might be a false alarm. This stark contrast underscores the critical role that background semantics play in assigning meaningful labels to visually similar objects.

However, it is crucial to highlight a significant gap in the current landscape of infrared small target detection research. Despite the availability of several public datasets, such as SIRST v1 [15] /v2 [4], NUDT-SIRST [16], and IRSTD1K [12], *none of these datasets provide detailed semantic annotations for the background regions*. To enable the explicit semantic modeling of backgrounds, a prerequisite is the creation of a dataset that includes background class annotations. Such

a dataset would provide a solid foundation for researchers to develop algorithms that can leverage the rich contextual information present in the background regions.

To address the aforementioned challenges, this study presents DenseSIRST, a new open-source infrared target detection benchmark dataset. Compared to previous datasets in this field, DenseSIRST has implemented two significant upgrades. *Firstly*, the dataset transitions from a simple sparse target detection task to the precise detection of dense, clustered targets, substantially increasing the task’s difficulty and practical value. *Secondly*, DenseSIRST performs detailed per-pixel semantic segmentation of the background, dividing it into sky and non-sky categories, thereby providing preliminary support for explicit semantic modeling of the background.

Building upon this foundation, we propose the Background-Aware Feature Exchange Network (BAFE-Net) framework, which transforms the infrared small target detection paradigm from a single target detection task that solely focuses on the foreground to a multi-task architecture that jointly performs target detection and background semantic segmentation. BAFE-Net introduces a cross-task feature hard-exchange module in the target detection head and background segmentation head, which embeds target semantics and background semantics between the segmentation and detection tasks through a feature adapter. *To the best of our knowledge, this paper is the first to propose a cross-task feature hard-exchange mechanism*. Benefiting from the explicit modeling of background semantics, BAFE-Net can better understand the contextual information in the scene, thereby significantly improving the accuracy of target detection and greatly reducing the false alarm rate.

Finally, by leveraging the fine-grained semantic annotations of the background, we propose a Background-Aware Gaussian Copy-Paste (BAG-CP) method. During the training phase, this method selectively pastes small targets into the sky region based on different background environments during data augmentation. This approach avoids pasting small targets into complex non-sky background regions, such as urban ground, which can produce highly similar false alarm targets.

In summary, our contributions can be categorized into

**THREE** main aspects:

- 1) We propose a new task—clustered infrared small target detection, and have released a new dataset, DenseSIRST, annotated with background semantic segmentation.
- 2) Utilizing DenseSIRST, we propose and demonstrate the effectiveness of the Background-Aware Gaussian Copy-Paste (BAG-CP) method, which outperforms the original Copy-Paste method that ignores background semantics.
- 3) We propose the BAFE-Net, which achieves a learning mechanism of mutual promotion between segmentation and detection tasks by implementing feature hard-exchange with a cross-task adapter, based on explicit background modeling.

To validate the effectiveness of BAG-CP and BAFE-Net, we provide extensive experimental results demonstrating their ability to improve the accuracy of target detection while reducing the false alarm rate. The experimental results demonstrate that our method outperforms the compared methods, showcasing its superior performance.

## II. RELATED WORK

### A. Infrared Small Target Detection

Infrared small target detection methods can be primarily categorized into model-driven and data-driven methods. Model-driven methods can be broadly categorized into three subclasses, each incorporating different strategies to model the relationship between targets and backgrounds.

- 1) *Background Estimation Methods*: These include techniques like Top-hat filtering [17] and Max-Median filtering [18]. By leveraging the local consistency of backgrounds, these methods construct filters to enhance target visibility. However, they falter when dealing with extremely weak targets, leading to missed detections and a high sensitivity to hyperparameters. The primary limitation stems from insufficient semantic understanding of the features, which often results in poor performance in complex backgrounds and increased false alarms.
- 2) *Human Visual System (HVS) Methods*: Techniques such as local contrast measure (LCM) [7] and multi-scale patch-based contrast measure (MPCM) [19] attempt to emulate the high spatial local contrast sensitivity of the human eye. Despite their intuitive appeal, these methods struggle with very small or blurred targets, mainly due to their inability to generate sufficient contrast.
- 3) *Low-Rank and Sparse Decomposition (LRSD) Methods*: This category includes approaches like the infrared patch-image model (IPI) [5], partial sum of tensor nuclear norm (PSTNN) [20], and sparse regularization-based twisted tensor model. These methods have gained popularity for their robustness in target and background separation. However, they severely suffer from the challenge of distinguishing background distractors from targets due to the similar sparse characteristic.

Despite their contributions, these methods suffer from several limitations, including poor performance in complex backgrounds, high false alarm rates, and sensitivity to hyperparameters, which we attribute to the lack of feature semantics.

Transitioning from model-driven methods, data-driven approaches have revolutionized the field by leveraging neural networks to automatically extract and learn features relevant for detecting small targets. Methods such as asymmetric context modulation (ACM) [15], dense nested attention networks (DNANet) [16], and gated shaped trans u-net (GSTUnet) [11] have shown significant promise. These methods concentrate on integrating the features of infrared small targets with neural networks, often utilizing deeper neural networks or more robust attention modules. The advantages of data-driven methods lie in their ability to automatically extract features and focus on multi-scale feature interaction, which can be seen as a form of *implicit modeling of the relationship between targets and background*.

While effective to a degree, these methods treat all backgrounds as a single class, ignoring the significant impact of different background semantics on distinguishing between true targets and false alarms with similar appearances. Moreover, despite not fully depending on sparse priors or local contrast priors like traditional methods, some approaches still leverage this prior knowledge to enhance detection performance. Their performance is greatly affected in dense scenes with multiple adjacent targets, where the assumption of local contrast between targets and their neighboring background no longer holds. This fundamental shift in target distribution necessitates the development of approaches that can effectively handle the complex interactions and dependencies among multiple targets in close proximity.

In contrast to previous studies, our work addresses several key limitations and explores new frontiers in infrared small target detection:

- 1) **Focusing on the Unexplored Challenge of Clustered Targets**: Unlike traditional approaches that primarily focus on isolated targets, we take on the more complex task of detecting clustered targets, introducing a new challenge in this field. We further facilitate the research in this area by providing DenseSIRST, a dedicated dataset created specifically for this novel task.
- 2) **Incorporation of Explicit Semantic Modeling with DenseSIRST**: In contrast to previous studies that often treat all backgrounds as a homogeneous class, we leverage the DenseSIRST dataset’s semantic segmentation annotations for background modeling. Our proposed BAFE-Net thereby gains an enhanced understanding of the target’s background, leading to improved detection accuracy.
- 3) **Introduction of Cross-Task Feature Exchange**: Our cross-task feature exchange module brings together background semantics and target features through a feature adapter, *a strategy not commonly found in existing work*. This approach enables a more precise differentiation between targets and their backgrounds.

### B. Data Augmentation for Object Detection

Data augmentation is pivotal in enhancing the performance and generalization of object detection models. By diversifying training data through various transformations such as flipping, rotation, scaling, and cropping, models learn to recognize

and generalize across a broader spectrum of object variations. However, while these basic techniques are widely used, they often fall short in complex detection scenarios, necessitating more sophisticated methods.

To address the limitations of traditional methods, advanced augmentation techniques have been developed, which introduce more nuanced transformations that better preserve and highlight essential features of the objects while still enhancing the dataset’s diversity. For instance, CutMix [21] improves upon the CutOut [22] method by overlaying a segment of one image onto another, blending labels proportionally to the area of the patch, thereby maintaining more contextual integrity. Attentive-CutMix [23] refines this approach by selecting regions based on feature importance, thus preserving significant target details. SnapMix [24] and SaliencyMix [25] adjust the blending process based on saliency or importance maps, aiming to preserve crucial features while enhancing background complexity. TransMix [26] integrates attention mechanisms to better manage the blending of features, focusing on maintaining important target characteristics during augmentation. StyleMix [27] and PuzzleMix [28] introduce style and structural considerations into the mix, allowing for more complex transformations that consider both content and style elements of the images, potentially offering more robust augmentation strategies.

Despite these advancements, these methods primarily assume the presence of larger, easily distinguishable targets and do not specifically cater to the unique challenges posed by clustered infrared small target detection. None of these methods are explicitly designed to handle the high-density and occlusion-prone nature of infrared small targets. This gap highlights the need for augmentation strategies that directly address the intricacies of detecting small, closely-spaced targets against complex backgrounds.

Where our methodology aligns with the broader goal of enhancing infrared small target detection, it stands out in its unique focus and innovative strategies:

- 1) **Pioneering Data Augmentation for Clustered Infrared Small Target Detection:** Uniquely, our method pioneers a data augmentation technique specifically tailored for clustered infrared small target detection. It takes into account the local contrast prior and enables dynamic random variations in local contrast, a perspective not often considered in existing techniques.
- 2) **Context-Aware Target Placement:** Our proposed BAG-CP approach diverges from the commonly used random or fixed-position copy-paste tactics. Instead, it integrates background semantics to guide target placement, thereby skirting potential category conflicts induced by inconsistent background contextual semantics. This nuanced approach to the distinctive challenges in infrared small target detection tasks sets our work apart.

### C. Multi-Task Learning and Cross-Task Mechanism

Multi-task learning (MTL) is a pivotal strategy in computer vision that enhances model performance and generalization by jointly learning related tasks, such as detection and segmentation. By learning shared representations from multiple

supervisory tasks, MTL has shown remarkable success in the field of recognition.

Recent studies have introduced novel architectures and mechanisms to bolster the capabilities of MTL in object detection. Takikawa *et al.* [29] introduced a two-stream CNN architecture for semantic segmentation that explicitly wires shape information as a separate processing branch, using gates to connect the intermediate layers of the two streams. Misra *et al.* [30] proposed a new sharing unit called “cross-stitch” unit, which combines activations from multiple networks and can be trained end-to-end to learn an optimal combination of shared and task-specific representations. Zhang *et al.* [12] developed ISNet, which employs a Taylor finite difference (TFD)-inspired edge block and two-orientation attention aggregation (TOAA) block to enhance edge information and capture shape characteristics of infrared small targets.

However, these methods may not be well-suited for clustered infrared small target detection, as they often rely on edge detection or surface normal estimation, which assume larger targets. In real-world scenarios, infrared small targets typically consist of only 1-9 pixels and are subject to the diffusion effect, lacking clear edges and falling far below the conventional definitions of small targets, *i.e.*,  $32 \times 32$  pixels in general object detection.

In this context, cross-task mechanisms that enable feature exchange between different tasks are more relevant to our work. These methods enhance MTL by facilitating feature exchange or distillation across different tasks, allowing each task to benefit from complementary signals of others. Methods like prediction-and-distillation network (PAD-Net) utilize attention-based mechanisms to distill multi-modal features effectively [31], while MTI-Net extends this concept with a multi-scale approach better suited for handling diverse task demands [32].

While our work builds upon the foundational principles of multi-task learning and cross-task mechanisms, it distinguishes itself in the feature hard-exchange mechanism. Diverging from the soft fusion approach used in attention-based methods, we employ a feature hard-exchange mechanism for feature fusion. This simple yet effective strategy ensures a more robust integration of features from different tasks.

## III. THE DENSESIRST DATASET

### A. Motivation and Rationale

The detection of small, low-contrast targets against complex backgrounds in infrared imagery is a significant challenge that impacts the performance of computer vision algorithms. While existing datasets have contributed to the advancement of this field, they often suffer from limitations such as sparse target distribution and a focus on larger target sizes, which do not adequately represent real-world scenarios.

To address these limitations, we introduce the DenseSIRST dataset, a richly annotated collection of infrared images featuring densely populated small targets. DenseSIRST not only increases the number of small targets per image but also encompasses a variety of target sizes and complex clustering, crucial for training and evaluating algorithms under realistic and challenging conditions.

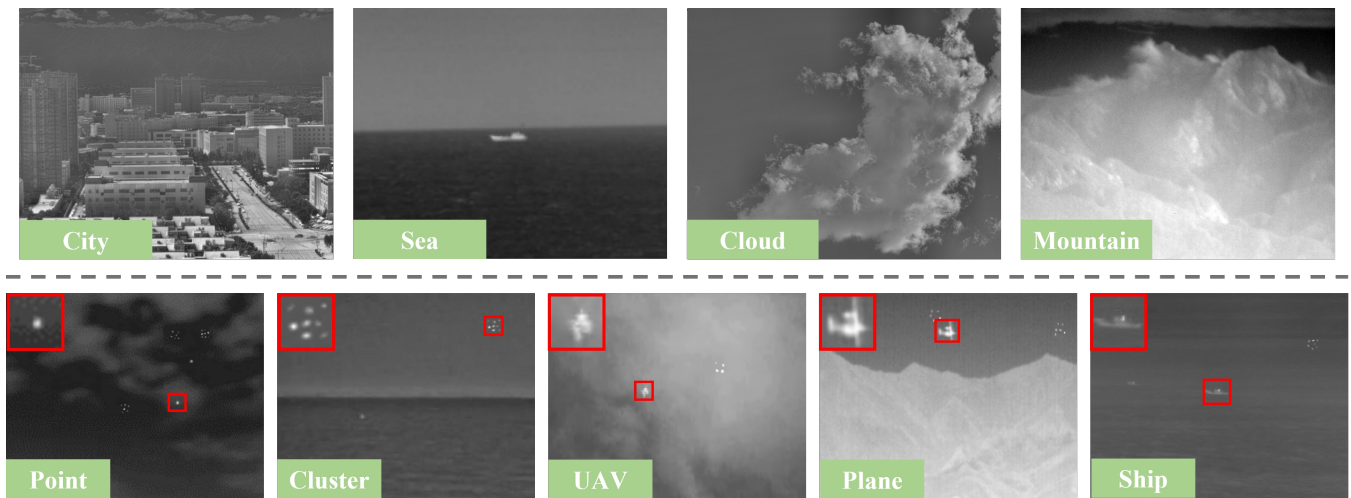


Fig. 2. The four images above show diverse backgrounds, including city, sea, cloud, and mountain. The five diagrams below illustrate various targets, including Point, Cluster, UAV, Plane, and Ship.

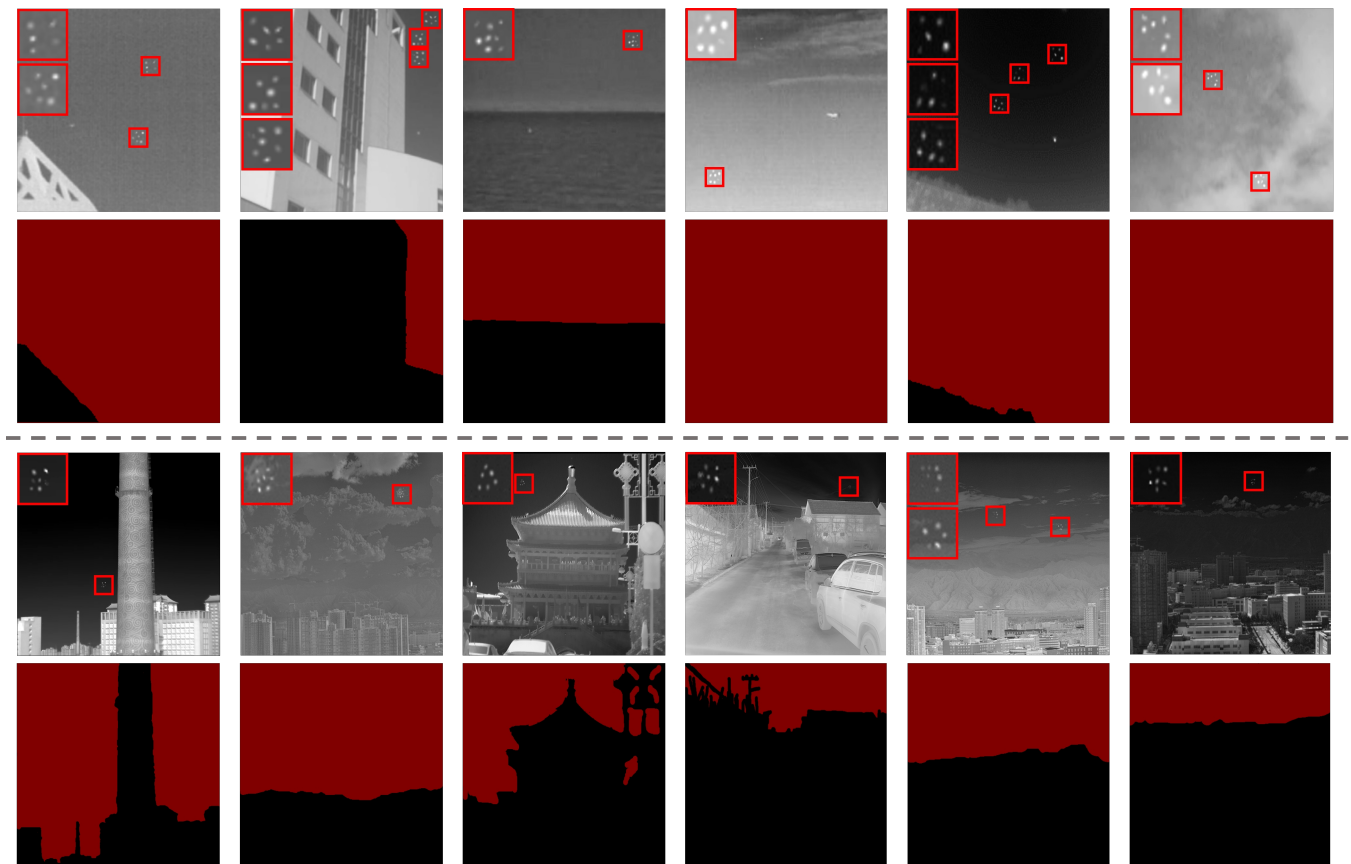


Fig. 3. A total of 12 dataset images are shown. In each set of images, the top figure shows the simulated dense small target, and the bottom figure shows the corresponding sky segmentation of the image.

TABLE I  
MAIN CHARACTERISTICS OF SEVERAL POPULAR SIRST DATASETS.

Datasets	Image Type	Annotation Type	Image Number	Target Number	Average Target Area	Sparse or Clustered	Background Semantic Annotation
SIRST [15]	Real	Pixel	427	533	23	Sparse	×
SIRSTv2 [4]	Real	Pixel + BBox + Point	1024	648	24	Sparse	×
IRSTDIK [12]	Real	Pixel	1001	1495	38	Sparse	×
SIRSTAUG [33]	Synthetic	Pixel	8525	9278	88	Sparse	×
<b>DenseSIRST (Ours)</b>	Real + Synthetic	Pixel + BBox + Point	1024	<b>13655</b>	<b>6</b>	<b>Cluster</b>	✓

Table I compares DenseSIRST with several well-regarded datasets, such as SIRST [15], SIRSTv2 [4], IRSTD1K [12], and SIRSTAUG [33]. These datasets predominantly feature sparsely distributed targets and lack comprehensive annotations for clustered small targets. In contrast, DenseSIRST distinguishes itself through:

- 1) **Hybrid Image Composition:** Combining real and synthetic targets, DenseSIRST enhances both the realism and diversity of the training data.
- 2) **Target Density and Diversity:** With an average target area significantly smaller than existing datasets and a higher number of targets per image, DenseSIRST provides a challenging scenario for detection algorithms.
- 3) **Variied Background Scenarios:** The dataset includes images from diverse backgrounds such as urban, mountainous, maritime, and cloudy scenes, as shown in Fig. 2, each contributing to the complexity of the detection tasks.

Fig. 3 showcases a selection of images from the DenseSIRST dataset, illustrating the dense distribution of small targets and the corresponding sky segmentation annotations. These annotations provide valuable contextual information for developing and evaluating detection algorithms.

### B. Target Synthesis and Composition

The DenseSIRST dataset, a blend of real and synthetic infrared images, provides a challenging and dense environment for training robust detection algorithms. We curated this dataset from diverse real-world scenarios, supplemented with synthetic targets designed for physical plausibility and visual realism.

The dataset leverages the existing SIRSTv2, creating a broad library of infrared small targets. Each image is meticulously designed to emulate the densely populated surveillance scenarios. Specifically, one to three “dense areas” are defined randomly within the less cluttered sky regions of each base image. These areas, each measuring  $20 \times 20$  pixels, are populated with 8 to 12 targets selected randomly from the target library. The selected targets are resized to dimensions within  $5 \times 5$  pixels to maintain scale variability and pasted with a spacing of 1 to 2 pixels between them to simulate realistic clustering.

To ensure a smooth integration of targets and their backgrounds, we employ a Gaussian-weighted copy-paste technique, an evolution of the concept from mixup. This modification is governed by the following equation:

$$T_{new} = T_{back} + B_{box} \times \lambda \times G, \lambda \in [0.5, 1] \quad (1)$$

Here,  $T_{new}$  denotes the adjusted target appearance, while  $T_{back}$  is the original background at the target’s location. Different from mixup, its weight is set to 1 for enhancing the reality of the synthesized target.  $B_{box}$  represents the original target appearance. The scalar  $\lambda$ , which adjusts the target’s brightness, is randomized to diversify the brightness and contrast of targets, thus enriching the sample space.

The matrix  $G$  denotes a Gaussian blur, employed during target pasting, and is defined as:

$$G(x, y) = e^{-\frac{(x-\rho_x w)^2}{2\sigma_x^2} - \frac{(y-\rho_y h)^2}{2\sigma_y^2}}, \quad (2)$$

The relative offsets  $\rho_x$  and  $\rho_y$  determine the Gaussian distribution center along the  $x$  and  $y$  axes, randomly selected within the range  $[0, 0.2]$ . These values, when multiplied by the target bounding box’s width  $w$  and height  $h$ , yield the actual pixel offsets, ensuring appropriate scaling with the target size. The Gaussian distribution’s spread is controlled by the standard deviations  $\sigma_x$  and  $\sigma_y$  along the  $x$  and  $y$  axes, randomized within  $[0.3, 0.6]$ . This randomness guarantees varying degrees of edge blurring among the simulated targets, reinforcing their realistic appearance.

To further enhance variability, each target undergoes a rotational transformation. The Gaussian matrix’s rotation  $\theta$  is applied as:

$$\begin{bmatrix} x' \\ y' \end{bmatrix} = \begin{bmatrix} \cos(\theta) & -\sin(\theta) \\ \sin(\theta) & \cos(\theta) \end{bmatrix} \begin{bmatrix} x - \mu_x \\ y - \mu_y \end{bmatrix}, \quad (3)$$

Here,  $\theta$  is randomly selected from the interval  $[-90^\circ, 90^\circ]$ .

### C. Dataset Description and Characteristics

1) **Composition of the Dataset:** The DenseSIRST dataset comprises 1024 infrared images, with a total of 13,655 densely clustered small targets. The images in the DenseSIRST dataset cover a wide range of realistic scenarios, including urban areas, mountainous regions, maritime environments, and cloudy scenes. This diversity enables the development and assessment of infrared small target detection algorithms that can generalize well to various real-world applications. The division of training set, validation set, and test set is aligned with the SIRSTv2 dataset.

2) **Annotations and Labels:** In the DenseSIRST dataset, each image is meticulously annotated with three types of labels: pixel-level masks, bounding boxes, and point annotations. The pixel-level masks provide precise segmentation of each target, enabling the evaluation of algorithms at a fine-grained level. Bounding box annotations encapsulate each target with a rectangular box, facilitating the assessment of detection performance using metrics such as precision, recall, and F1 score. Point annotations mark the center of each target, allowing for the evaluation of localization accuracy.

3) **Statistical Characteristics of the Dataset:** The DenseSIRST dataset is meticulously curated to provide a comprehensive benchmark for clustered infrared small target detection. This part offers a detailed analysis of the dataset’s key characteristics, including the distribution of image sizes, target sizes, local contrast, and brightness levels.

**Image Size Distribution:** The dataset, as depicted in Fig. 4 (a), includes images with resolutions ranging from  $320 \times 256$  to  $1280 \times 1024$  pixels, covering various typical infrared camera resolutions encountered in real-world scenarios. This diversity is crucial for developing detection algorithms that can generalize across different resolutions.

**Target Size Distribution:** Most targets, as indicated in Fig. 4 (b), are extremely small, predominantly below  $5 \times 5$  pixels. The  $3 \times 3$  pixels size is the most frequent, aligning with the characteristics of small target detection in infrared imagery. With a total of 13,655 annotated targets, the dataset provides a rich set of examples for training and evaluation.

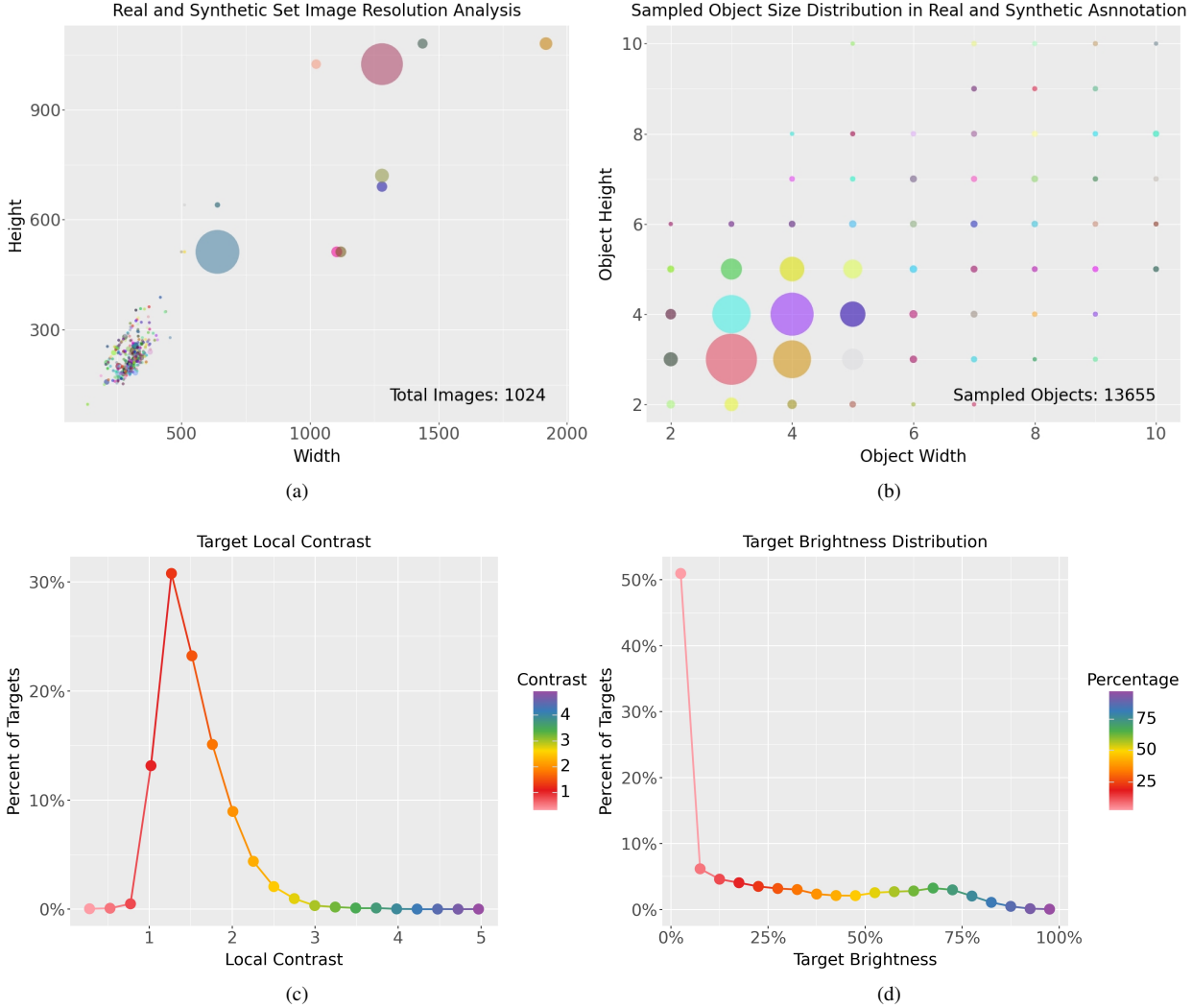


Fig. 4. Figure (a) is the image resolution characteristic, the larger the range of circles in the scatter plot, the greater the number of images at that resolution. Figure (b) is the target size characteristic, and the larger the range of circles in the scatter plot, the greater the number of small targets of that size. Figure (c) shows the percentage of different local contrasts for small objects in the dataset, with the lowest local contrast being 0.15. Figure (d) shows the percentage of brightness distribution for small targets in the dataset, and shows that the brightness distribution is wide from dark targets to light targets.

**Local Contrast Distribution:** The vast majority (90%) of targets have local contrast values below 2, as shown in Fig. 4 (c). This low contrast is indicative of the inherent difficulty in detecting such targets against cluttered backgrounds. Moreover, the presence of nearby targets within dense clusters can inadvertently be included in the background calculation, leading to an underestimation of local contrast and further complicating detection.

**Target Brightness Distribution:** Fig. 4 (d) reveals that only a minority of targets are the brightest points in their respective images. This characteristic emphasizes the inadequacy of brightness as a sole distinguishing feature for target detection in infrared images.

In conclusion, the DenseSIRST dataset, with its wide range of image dimensions, prevalence of small target sizes, and low local contrast, provides a realistic and challenging benchmark for infrared small target detection algorithms.

## IV. BACKGROUND-AWARE FEATURE EXCHANGE NETWORK

### A. Overall Architecture and Training Pipeline

The proposed BAFE-Net adopts a fully convolutional one-stage object detector (FCOS) [34] as its host network. FCOS is a simple yet effective anchor-free object detection framework that has demonstrated superior performance in various computer vision tasks. By leveraging the inherent advantages of FCOS, such as its ability to handle objects of different scales and aspect ratios without the need for predefined anchor boxes, BAFE-Net aims to address the challenges of detecting small, densely clustered targets in infrared imagery.

The overall architecture of BAFE-Net is illustrated in Fig. 5. In addition to the original detection head present in the baseline FCOS, BAFE-Net introduces a segmentation head within the BAFE-Head module. The primary purpose of incorporating this segmentation head is to enable explicit modeling of background semantics, which is crucial for enhancing the network's ability to distinguish between real targets and background clutter.

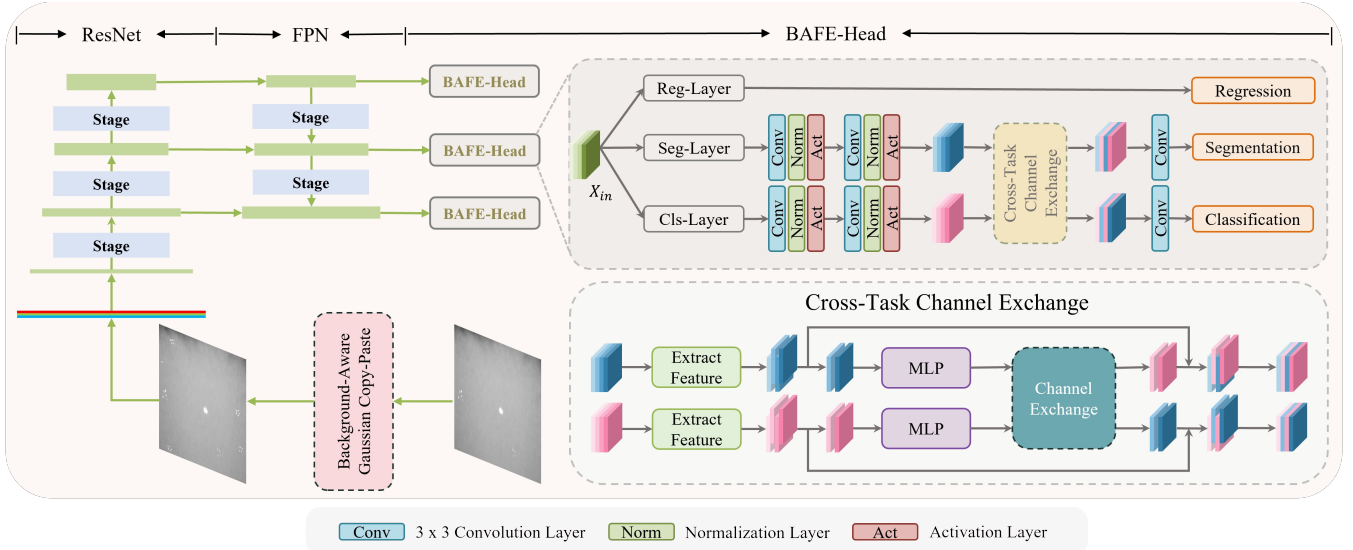


Fig. 5. Schematic diagram of the proposed BAFE-Net network. BAFE-Net contains three modules: ResNet, FPN and BAFE-Head.

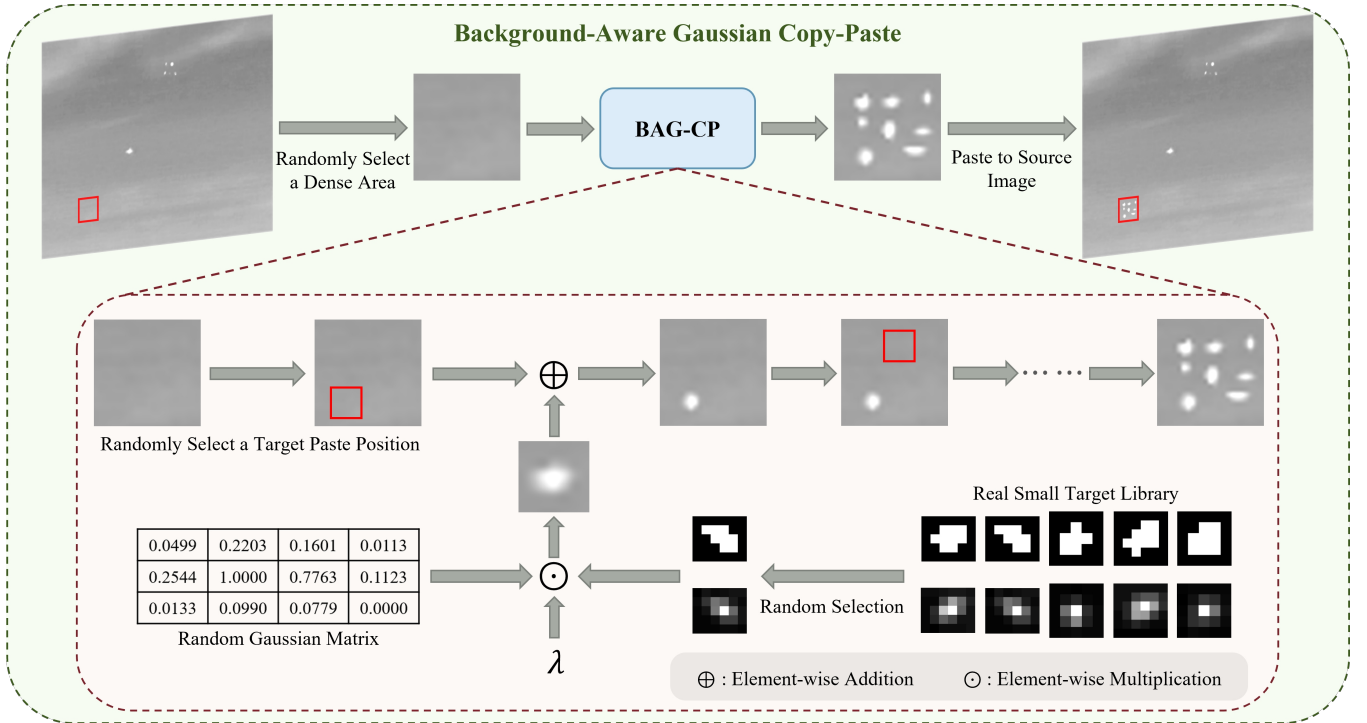


Fig. 6. First, a dense area is randomly selected from the sky area of the image, and then several small targets are randomly selected from the small target library. After determining the appropriate pasting position, the Gaussian technique is used to integrate the small targets into the new background.

in infrared scenes. By jointly optimizing the detection and segmentation tasks, BAFE-Net learns to capture both object-level and pixel-level contextual information, ultimately leading to improved detection performance.

In addition to the architecture modifications, BAFE-Net incorporates a novel training methodology termed Background-Aware Gaussian Copy-Paste (BAG-CP). This technique is used during the training phase to augment the training dataset with realistically integrated synthetic targets. BAG-CP strategically places synthetic infrared small targets into real scene backgrounds by considering semantic context, which significantly

enhances the training process. The use of Gaussian smoothing at the edges of the pasted targets ensures seamless integration, avoiding artificial boundary artifacts that could mislead the learning algorithm.

This context-aware synthesis and integration approach allows BAFE-Net to train on a dataset that closely mimics operational scenarios, where small targets often appear against complex and cluttered backgrounds. By training the network to recognize and handle these challenging conditions effectively, BAFE-Net sets a new standard for performance in infrared small target detection.



## B. Cross-Task Feature Exchange Module

During the feature extraction process, partial feature exchange is performed between segmentation and classification tasks within this network. The segmentation and classification tasks have different focuses when learning features: segmentation emphasizes local details and contextual information, whereas classification emphasizes global features. Despite their differing objectives, there is a potential synergistic relationship between segmentation and classification tasks. By exchanging features, information can be shared between the two tasks, promoting collaborative learning and enhancing the feature representation capabilities of each task. Segmentation can assist classification in better understanding the structure and semantics of the image, while classification can help segmentation in distinguishing boundaries and details of different categories. Specifically, segmentation features can leverage global information from classification features to improve overall understanding, while classification features can utilize local detail information from segmentation features to enhance precision. Mutual learning between segmentation and classification features can reduce the risk of overfitting and improve the model’s performance in practical applications. Feature exchange enables the model to perform more robustly when facing different tasks. It allows the model to better adapt to various changes and uncertainties, thereby enhancing its generalization ability across different scenarios.

Feature exchange has been proven feasible for several reasons: 1) **Complementarity of features**: Although segmentation and classification features are different, they are extracted from the same input image and thus possess a degree of complementarity. By exchanging features, each task can utilize useful information from the other task, thereby improving overall performance. 2) **Compatibility of features**: Deep learning models use continuous and differentiable operations, such as convolution and pooling, when extracting features. Through feature exchange, these operations can still ensure the coherence and differentiability of features, thus not disrupting the training process of the model. 3) **Support from existing research**: Some studies have already shown that in multi-task learning, sharing or exchanging features can improve the overall performance of tasks. For example, in the Changer [35] paper, channel and spatial exchanges were used and proven feasible.

Feature exchange primarily consists of two methods: channel exchange and spatial exchange. Channel exchange involves directly swapping features at the channel level between different feature maps, while spatial exchange is achieved by swapping features along the spatial dimensions of the feature maps. In the Cross-Task Feature Exchange Module, channel exchange is employed, and experiments have shown that channel exchange performs better than spatial exchange. The experimental results will be presented in Section V.

Assume  $x_1$  and  $x_2$  are the input tensors, each with a shape of  $(N, C, H, W)$ , where  $N$  is the batch size,  $C$  is the number of channels, and  $H$  and  $W$  are the height and width, respectively. Let  $p$  be a parameter controlling the proportion of channel exchange. Define an exchange mask  $E$  with a shape of  $C$ ,

$$E[i] = \begin{cases} 1 & , \text{ if } i \bmod \left(\frac{1}{p}\right) = 0 \\ 0 & \end{cases} \quad (4)$$

where  $i$  is the channel index. Expand the exchange mask  $E$  to the shape of  $(N, C, H, W)$ ,

$$E_{\text{expanded}} = E \otimes 1_{N \times H \times W} \quad (5)$$

where  $\otimes$  denotes the expansion operation, and  $1_{N \times H \times W}$  is a tensor of ones with a shape of  $(N, H, W)$ . Define the output tensors  $y_1$  and  $y_2$ ,

$$y_1 = x_1 \odot (1 - E_{\text{expanded}}) + x_2 \odot E_{\text{expanded}} \quad (6)$$

$$y_2 = x_2 \odot (1 - E_{\text{expanded}}) + x_1 \odot E_{\text{expanded}} \quad (7)$$

where  $\odot$  denotes element-wise multiplication.

However, the features to be exchanged are cross-modal. Therefore, an Adapter is introduced to process these features before the exchange. Here, an MLP (Multi-Layer Perceptron) is used as the Adapter. The features to be exchanged are fed into the Adapter separately, and after processing, the features are exchanged. This approach addresses the cross-modal issue between the features.

## C. Background-Aware Gaussian Copy-Paste

Infrared small target detection is inherently challenged by the paucity of intrinsic visual features in targets and the interference from similar background elements. Traditional data augmentation strategies, such as random cropping or flipping, are not effective in addressing these unique challenges. Consequently, we propose a novel data augmentation technique, Background-Aware Gaussian Copy-Paste (BAG-CP), which capitalizes on contextual information to enhance the training process. BAG-CP selectively augments training images by pasting infrared small targets into semantically relevant background areas, generating more realistic and diverse training samples. The fundamental idea is to bolster the detector’s ability to discern real targets from background noise through the seamless blending of pasted targets into their new environment. As illustrated in Fig. 6, The BAG-CP process unfolds as follows:

**Prerequisite: Semantic Annotation of Background**: Before performing the copy-paste operation, it is crucial to have the image segmented into different semantic regions. The DenseSIRST dataset includes annotated background categories, providing detailed background masks that separate sky from non-sky regions.

**Step 1: Selection and Extraction of Infrared Small Targets**: A library of small targets is created during the generation of the DenseSIRST dataset. A random selection of small targets from this library is made for pasting into the current training image.

**Step 2: Gaussian Smoothing of Edges**: Prior to pasting, the selected targets are subjected to Gaussian smoothing. This step ensures a smooth transition around the pasted targets, minimizing any conspicuous artifacts that might disrupt the learning process.

**Step 3: Context-Aware Target Pasting Based on Background Semantics:** The core of BAG-CP lies in context-aware placement. Using the semantic annotation of the background, we classify it into sky and non-sky regions. When choosing where to paste the Gaussian-smoothed targets, we only select locations within the sky regions. This approach mimics real-world scenarios where infrared small targets, especially aerial targets, are more likely to appear against a sky background.

During the pasting process, 1-3 regions are selected within the image to form clusters of small targets. Each region is  $20 \times 20$  pixels in size and is populated with 8 to 12 targets randomly chosen from the target library. The selected targets are resized to within  $5 \times 5$  pixels to maintain proportional variability and are pasted with a spacing of 1 to 2 pixels to simulate realistic clustering. The Gaussian-weighted edge blurring technique used follows Eq. (1), Eq. (2), and Eq. (3).

## V. EXPERIMENTS

In this section, we outline a series of experimental evaluations designed to validate the effectiveness of the Background-Aware Gaussian Copy-Paste (BAG-CP) method and the Background-Aware Feature Exchange Network (BAFE-Net) proposed in this study. Additionally, we conduct comparative analyses with state-of-the-art methods in infrared small target detection, using both quantitative metrics and qualitative assessments. We address the following pivotal questions in our experimental analysis:

- 1) **Ablation Study on Background-Aware Gaussian Copy-Paste.** We compare the performance of various copy-paste strategies to demonstrate the superiority of our BAG-CP method.
- 2) **Effectiveness of Background-Aware Feature Exchange.** We evaluate the performance of BAFE-Net by comparing different configurations to highlight the contributions of each component in BAFE-Net.
- 3) **Feature Exchange Mechanism Analysis.** We investigate the impact of different feature exchange strategies on the performance of BAFE-Net to determine the optimal approach for exchanging features between the target detection head and the background segmentation head.
- 4) **Impact of Backbone Depth:** We examine the influence of varying backbone depths on the performance of the BAFE-Net. The primary aim is to establish the optimal depth that maximizes target detection while balancing computational efficiency.
- 5) **Comparative Analysis with State-of-the-Art Methods.** We conduct a comprehensive comparison between our method and other state-of-the-art methods on the DenseSIRST dataset.

### A. Experimental Settings

1) **Dataset:** During the experimental phase of our research, we conducted tests on the proposed dataset DenseSIRST.

2) **Implementation Details:** Our network was trained on an NVIDIA RTX 3090 GPU platform with 24GB of memory. In our experiments, we employed the DeepInfrared toolkit for object detection. Considering the image sizes in the dataset and computational overhead, for methods within the DeepInfrared

toolkit, we set the range of the long edge of training and testing images to [512, 512] while maintaining aspect ratio to avoid image distortion. We choose FocalLoss as the loss function of the classification branch, IoULoss as the loss function of the regression branch, and CrossEntropyLoss as the loss function of the segmentation branch. We choose DAdaptAdam as the optimizer, lr is set to 1.0, and weight decay is set to 0.05. Considering training and convergence time, we trained for 20 epochs within the DeepInfrared framework. Through experimentation, we observed that different parameter settings affect the detection efficacy of dense small objects. Thus, while ensuring basic fairness, we adjusted the parameters of different methods to obtain optimal detection results.

3) **Evaluation Metrics:** We used mean Average Precision (mAP) with IoU thresholds of 0.5 ( $mAP_{0.7}$ ) and 0.75 ( $mAP_{12}$ ), and Recall as evaluation metrics for our experiment. They are defined as:

$$\text{mAP} = \frac{1}{N} \sum_{i=1}^N \text{AP}(i), \quad (8)$$

$$\text{AP} = \int_0^1 p(r) dr, \quad (9)$$

$$\text{Recall} = \frac{TP}{TP + FN}, \quad (10)$$

Here,  $N$  is the total number of samples,  $TP$ ,  $FP$ , and  $FN$  denote the number of true positive, false positive, and false negative instances, respectively. Precision  $p(r)$  is defined as the proportion of true positive detections out of the total number of positive detections at a given recall level  $r$ .

### B. Ablation Study

1) **Ablation Study on Background-Aware Gaussian Copy-Paste:** In this study, we initiate our investigation from the data augmentation module, focusing on the progressive integration of our proposed Copy-Paste technique, clustering of pasted objects, Gaussian module, and Background-Aware pasting. Our aim is to empirically validate the enhancements to detection performance brought about by these steps. To achieve this, we explore various combinations of the aforementioned components and conduct experimental validation of the results.

The experimental outcomes, as outlined in Table II, generate several key insights, providing a holistic understanding of the impact of each module. Firstly, the effective enhancement of detection performance by each module is noticeable, corroborating the initial motivation of our study. The Copy-Paste technique, even when used independently, significantly boosts performance, as evidenced by the increases of 1.1% and 2.3% on the DenseSIRST dataset, when comparing strategy (a) with strategy (b).

Further refinement through clustering of pasted objects also yields substantial improvements. This is evident when comparing strategies (b) to (c), and (d) to (e), respectively, indicating the considerable value of object clustering. Applying Gaussian blur to the edges of the pasted objects, as a means

TABLE II

QUANTITATIVE ABLATION STUDY EVALUATES THE IMPACT OF THE COPY-PASTE TECHNIQUE, CLUSTERING OF PASTED OBJECTS, GAUSSIAN MODULE, AND BACKGROUND-AWARE PASTING WITHIN THE DATA AUGMENTATION MODULE OF BAFE-NET

Strategy	Module				DenseSIRST			
	Copy-Paste	Cluster	Gaussian	Background-Aware	mAP <sub>07</sub> ↑	recall <sub>07</sub> ↑	mAP <sub>12</sub> ↑	recall <sub>12</sub> ↑
(a)	×	×	×	×	0.225	0.311	0.180	0.314
(b)	✓	×	×	×	0.236	0.322	0.203	0.303
(c)	✓	✓	×	×	0.242	0.329	0.205	0.335
(d)	✓	×	✓	×	0.245	0.321	0.211	0.338
(e)	✓	✓	✓	×	0.250	0.319	0.215	0.315
(f)	✓	✓	✓	✓	<b>0.258</b>	<b>0.340</b>	<b>0.220</b>	<b>0.340</b>

TABLE III

QUANTITATIVE ABLATION STUDY EVALUATES THE IMPACT OF THE BACKGROUND-AWARE SEGMENTATION, FEATURE EXCHANGE MODULE, AND ADAPTER MODULE WITHIN THE BACKGROUND-AWARE FEATURE EXCHANGE NETWORK (BAFE-NET)

Strategy	Module			DenseSIRST			
	Seg Head	Feature Exchange	Adapter	mAP <sub>07</sub> ↑	recall <sub>07</sub> ↑	mAP <sub>12</sub> ↑	recall <sub>12</sub> ↑
(a)	×	×	×	0.225	0.311	0.180	0.314
(b)	✓	×	×	0.246	0.324	0.183	0.304
(c)	✓	✓	×	0.254	0.321	0.199	0.310
(d)	✓	✓	✓	<b>0.262</b>	<b>0.318</b>	<b>0.208</b>	<b>0.305</b>

TABLE IV

QUANTITATIVE ABLATION STUDY WAS CONDUCTED TO EVALUATE THE IMPACT OF THE NUMBER OF HIDDEN LAYERS IN THE ADAPTER

Strategy	Hidden layers	DenseSIRST			
		mAP <sub>07</sub> ↑	recall <sub>07</sub> ↑	mAP <sub>12</sub> ↑	recall <sub>12</sub> ↑
(a)	8	0.222	0.305	0.206	0.308
(b)	16	0.243	0.318	0.214	0.310
(c)	32	0.256	0.329	0.218	0.312
(d)	64	<b>0.266</b>	<b>0.336</b>	<b>0.230</b>	<b>0.323</b>

TABLE V

QUANTITATIVE ABLATION STUDY EVALUATES THE IMPACT OF DIFFERENT FEATURE EXCHANGE MECHANISMS WITHIN THE FEATURE EXCHANGE MODULE OF BAFE-NET

Strategy	Exchange Method	DenseSIRST			
		mAP <sub>07</sub> ↑	recall <sub>07</sub> ↑	mAP <sub>12</sub> ↑	recall <sub>12</sub> ↑
(a)	Channel	<b>0.266</b>	<b>0.336</b>	<b>0.230</b>	<b>0.323</b>
(b)	Spatial	0.223	0.304	0.218	0.322
(c)	Channel + Spatial	0.246	0.310	0.199	0.314
(d)	Spatial + Channel	0.224	0.310	0.201	0.328

to enhance their realistic appearance, also proves to be significantly beneficial in improving detection performance. This is substantiated when comparing strategies (b) with (d), and (c) with (e).

Finally, the culmination of all modules in a Background-Aware Gaussian Copy-Paste context, as depicted by strategy (f), results in further enhancements in detection capability. This is demonstrated with an additional increase of 0.8% on the DenseSIRST dataset when comparing strategy (e) with strategy (f).

2) *Ablation Study on the Scheme of Background-Aware Feature Exchange*: The Background-Aware Feature Exchange module constitutes the core contribution of this paper, as

evidenced by its significant impact on detection performance demonstrated in Table III. To validate the effectiveness of the proposed components, we conducted an extensive ablation study by exploring various combinations of the background-based segmentation, Feature Exchange module, and adapter module.

Table III encapsulates the results of our experimental study and yields several crucial insights. Firstly, each constituent module substantively and independently enhances the detection performance, thereby validating the underpinnings of our research. Secondly, comparison between Strategy (a) and Strategy (b) reveals a significant performance augmentation when background-based segmentation is incorporated into

TABLE VI

QUANTITATIVE ABLATION STUDY EVALUATES THE IMPACT OF DIFFERENT BACKBONES ON BAFE-NET PERFORMANCE

Strategy	ResNet	DenseSIRST			
		mAP <sub>07</sub> ↑	recall <sub>07</sub> ↑	mAP <sub>12</sub> ↑	recall <sub>12</sub> ↑
(a)	ResNet18	0.258	0.328	0.233	0.341
(b)	ResNet34	0.258	0.330	0.226	0.332
(c)	ResNet50	<b>0.270</b>	<b>0.332</b>	<b>0.236</b>	<b>0.329</b>
(d)	ResNet101	0.256	0.324	0.241	0.336

TABLE VII  
COMPARISON WITH OTHER STATE-OF-THE-ART METHODS ON DENSESIRST.

Method	Backbone	DenseSIRST					
		mAP <sub>07</sub> ↑	recall <sub>07</sub> ↑	mAP <sub>12</sub> ↑	recall <sub>12</sub> ↑	Flops ↓	Params ↓
<i>One-stage</i>							
FCOS [34]	ResNet50	0.232	0.315	0.204	0.324	50.291G	32.113M
SSD [36]		0.211	0.421	0.178	0.424	87.552G	23.746M
GFL [37]	ResNet50	0.253	0.332	0.230	0.317	52.296G	32.258M
ATSS [38]	ResNet50	0.248	0.327	0.202	0.326	51.504G	32.113M
CenterNet [39]	ResNet50	0.000	0.000	0.000	0.000	50.278G	32.111M
PAA [40]	ResNet50	0.255	0.545	0.228	0.551	51.504G	32.113M
PVT-T [41]		0.109	0.481	0.093	0.501	41.623G	21.325M
RetinaNet [42]	ResNet50	0.114	0.510	0.086	0.523	52.203G	36.330M
EfficientDet [43]		0.099	0.433	0.072	0.419	34.686G	18.320M
TOOD [13]	ResNet50	0.256	0.355	0.226	0.342	50.456G	32.018M
VFNet [44]	ResNet50	0.253	0.336	0.214	0.336	48.317G	32.709M
YOLOF [45]	ResNet50	0.091	0.009	0.002	0.009	25.076G	42.339M
AutoAssign [46]	ResNet50	0.255	0.354	0.180	0.314	50.555G	36.244M
DyHead [47]	ResNet50	0.249	0.335	0.189	0.328	27.866G	38.890M
<i>Two-stage</i>							
Faster R-CNN [48]	ResNet50	0.091	0.022	0.015	0.029	0.759T	33.035M
Cascade R-CNN [49]	ResNet50	0.136	0.188	0.139	0.194	90.978G	69.152M
Dynamic R-CNN [50]	ResNet50	0.184	0.235	0.111	0.190	63.179G	41.348M
Grid R-CNN [51]	ResNet50	0.091	0.018	0.025	0.037	0.177T	64.467M
Libra R-CNN [52]	ResNet50	0.141	0.142	0.085	0.120	63.990G	41.611M
<i>End2End</i>							
DETR [53]	ResNet50	0.000	0.000	0.000	0.000	24.940G	41.555M
Deformable DETR [54]	ResNet50	0.024	0.016	0.018	0.197	51.772G	40.099M
DAB-DETR [55]	ResNet50	0.005	0.054	0.000	0.001	28.939G	43.702M
Conditional DETR [56]	ResNet50	0.000	0.000	0.000	0.001	27.143G	40.297M
Sparse R-CNN [57]	ResNet50	0.183	0.572	0.154	0.614	45.274G	0.106G
★ <b>BAFE-Net (Ours)</b>	ResNet50	<b>0.270</b>	0.332	<b>0.236</b>	0.329	69.114G	35.329M

object detection, wherein the detection head interacts with the segmentation head. This integration accounted for an increase of 1.0% and 0.3% on the DenseSIRST dataset.

Further, juxtaposition of Strategy (b) and Strategy (c) highlights the contribution of the Feature Exchange in the interaction mode between the detection head and the segmentation head. This interaction led to a notable improvement in detection performance by 1.1% on the DenseSIRST dataset. Upon comparing Strategy (c) and Strategy (d), it becomes evident that introducing feature adaptation prior to the Feature Exchange further amplifies detection performance.

As the feature adapter employs a Multi-Layer Perceptron (MLP), the number of hidden layers in the MLP is a crucial parameter that warrants careful consideration. Increasing the number of hidden layers typically improves performance but comes at the cost of increased computational complexity. To strike a balance between performance and efficiency, we conducted an experiment to determine the optimal number of hidden layers, as shown in Table IV. The experimental results demonstrate that increasing the number of hidden layers leads to a consistent improvement in detection performance. However, the performance gain becomes less significant when the number of hidden layers exceeds 64, while the parameter count increases substantially. Therefore, we opted for 64 hidden layers in the Adapter, as it provides a significant performance boost while maintaining a reasonable computational overhead

compared to using 128 hidden layers or more.

3) *Ablation Study on Feature Exchange Mechanism*: In this part, a rigorous exploration of various Feature Exchange Mechanisms was undertaken. This encompassed diverse mechanisms such as Channel Exchange and Spatial Exchange, along with a multitude of their combinations. The quest was to ascertain the most efficacious method for Feature Exchange. Channel Exchange, as a mechanism, facilitates the direct interplay at the channel level amongst different features. In contrast, Spatial Exchange is implemented by orchestrating exchanges along the spatial dimensions inherent in the feature maps. The exchange ratio was judiciously set at 0.5 to maintain a balance.

As delineated in Table V, the superiority of the Channel Exchange method over alternative Feature Exchange mechanisms is clearly manifested. The empirical evidence underscores the robustness and optimality of Channel Exchange, thereby validating its adoption as the preferred method for Feature Exchange in our model.

4) *Impact of Backbone Depth*:: For infrared small target detection, the depth of the backbone network emerges as a critical factor. A shallower network, while computationally efficient, might extract features with insufficient semantic richness, thereby impinging on the overall detection performance. Conversely, an excessively deep network might overwhelm the delicate features of smaller targets amidst the background,

consequently leading to a performance degradation.

We conducted a series of experiments using different ResNet architectures, varying the depth from ResNet18 to ResNet101, to identify the optimal backbone for our proposed BAFE-Net. The results of these experiments are summarized in Table VI. Notably, ResNet50 emerged as the most suitable backbone for the BAFE-Net.

### C. Comparison with State-of-the-Arts

We benchmarked our BAFE-Net against current leading or state-of-the-art methods on the proposed DenseSIRST dataset, using metrics such as  $mAP_{07}$ ,  $mAP_{12}$ , and Recall. The experimental results are presented in Table VII.

End-to-end (End2End) methods, while theoretically appealing due to their NMS-free style, demonstrated suboptimal performance. This can be attributed to their inherent requirement for extensive training data, akin to COCO-level volumes, for effective operation. The relatively limited availability of infrared small target detection datasets inherently handicaps such methods, resulting in their diminished performance.

Next, we observed that two-stage methods underperformed compared to one-stage methods. Two-stage methods generate candidate regions based on deeper features, which are then subjected to classification and bounding box regression. However, the DenseSIRST dataset, characterized by small and densely clustered infrared targets, poses a challenge for such methods, leading to their suboptimal performance.

In contrast, one-stage methods, which directly regress bounding boxes and categories on the feature pyramids, demonstrated superior performance. These methods are not only faster and more computationally efficient, but also achieved higher mAP and recall, indicating their overall effectiveness. Significantly, our BAFE-Net method outperformed all other one-stage methods. The superior performance of BAFE-Net validates the efficacy of our approach in accurately detecting small infrared targets amidst dense conditions.

### D. Visual Analysis

To further validate the effectiveness of our proposed methods, we conduct a visual analysis by comparing the feature activation maps of our approach with those of the top-performing competing methods in the quantitative evaluation. Fig. 7 illustrates the feature activation maps of the five most competitive methods, including our own, on representative samples from the DenseSIRST dataset.

From the visual results, we observe that our method exhibits two key advantages over the other approaches. First, the feature activation maps of our method demonstrate significantly stronger activation intensities in the target regions, indicating a higher sensitivity to the presence of infrared small targets. The deeper activation levels in the target areas suggest that our method is more effective in capturing the discriminative features of the targets, contributing to improved detection accuracy.

Second, our method generates cleaner background activation maps compared to the other methods. As evident from Fig. 7,

the background regions in our activation maps exhibit consistently lower activation intensities, effectively suppressing background interference. This can be attributed to the background-aware mechanism employed by BAFE-Net, which learns to differentiate between target and background regions during the feature exchange process. By minimizing the activation levels in the background areas, our method demonstrates enhanced robustness against false positives, leading to a higher detection precision.

## VI. CONCLUSION

This study tackles the key challenges in infrared small target detection by leveraging background semantics. We introduce DenseSIRST, a benchmark dataset with detailed background annotations, enabling the transition from sparse to dense target detection. Building upon this, we propose BAFE-Net, a multi-task architecture that explicitly models background semantics and facilitates cross-task feature hard-exchange. Moreover, we develop BAG-CP, a data augmentation method that selectively pastes targets into sky regions, outperforming the original Copy-Paste method. Extensive experiments validate the effectiveness of BAFE-Net and BAG-CP in improving detection accuracy and reducing false alarms. Our work underscores the importance of explicitly leveraging contextual information in infrared small target detection and paves the way for the development of more robust and context-aware algorithms in this domain.

## REFERENCES

- [1] M. Zhao, W. Li, L. Li, J. Hu, P. Ma, and R. Tao, "Single-frame infrared small-target detection: A survey," *IEEE Geoscience and Remote Sensing Magazine*, vol. 10, no. 2, pp. 87–119, 2022. 1
- [2] H. Deng, X. Sun, M. Liu, C. Ye, and X. Zhou, "Small infrared target detection based on weighted local difference measure," *IEEE Transactions on Geoscience and Remote Sensing*, vol. 54, no. 7, pp. 4204–4214, 2016. 1
- [3] Y. Han, J. Liao, T. Lu, T. Pu, and Z. Peng, "Kcpnet: Knowledge-driven context perception networks for ship detection in infrared imagery," *IEEE Transactions on Geoscience and Remote Sensing*, vol. 61, pp. 1–19, 2022. 1
- [4] Y. Dai, X. Li, F. Zhou, Y. Qian, Y. Chen, and J. Yang, "One-stage cascade refinement networks for infrared small target detection," *IEEE Transactions on Geoscience and Remote Sensing*, vol. 61, pp. 1–17, 2023. 1, 2, 5, 6
- [5] C. Gao, D. Meng, Y. Yang, Y. Wang, X. Zhou, and A. G. Hauptmann, "Infrared patch-image model for small target detection in a single image," *IEEE transactions on image processing*, vol. 22, no. 12, pp. 4996–5009, 2013. 1, 3
- [6] Y. Dai and Y. Wu, "Reweighted infrared patch-tensor model with both nonlocal and local priors for single-frame small target detection," *IEEE journal of selected topics in applied earth observations and remote sensing*, vol. 10, no. 8, pp. 3752–3767, 2017. 1
- [7] C. P. Chen, H. Li, Y. Wei, T. Xia, and Y. Y. Tang, "A local contrast method for small infrared target detection," *IEEE*

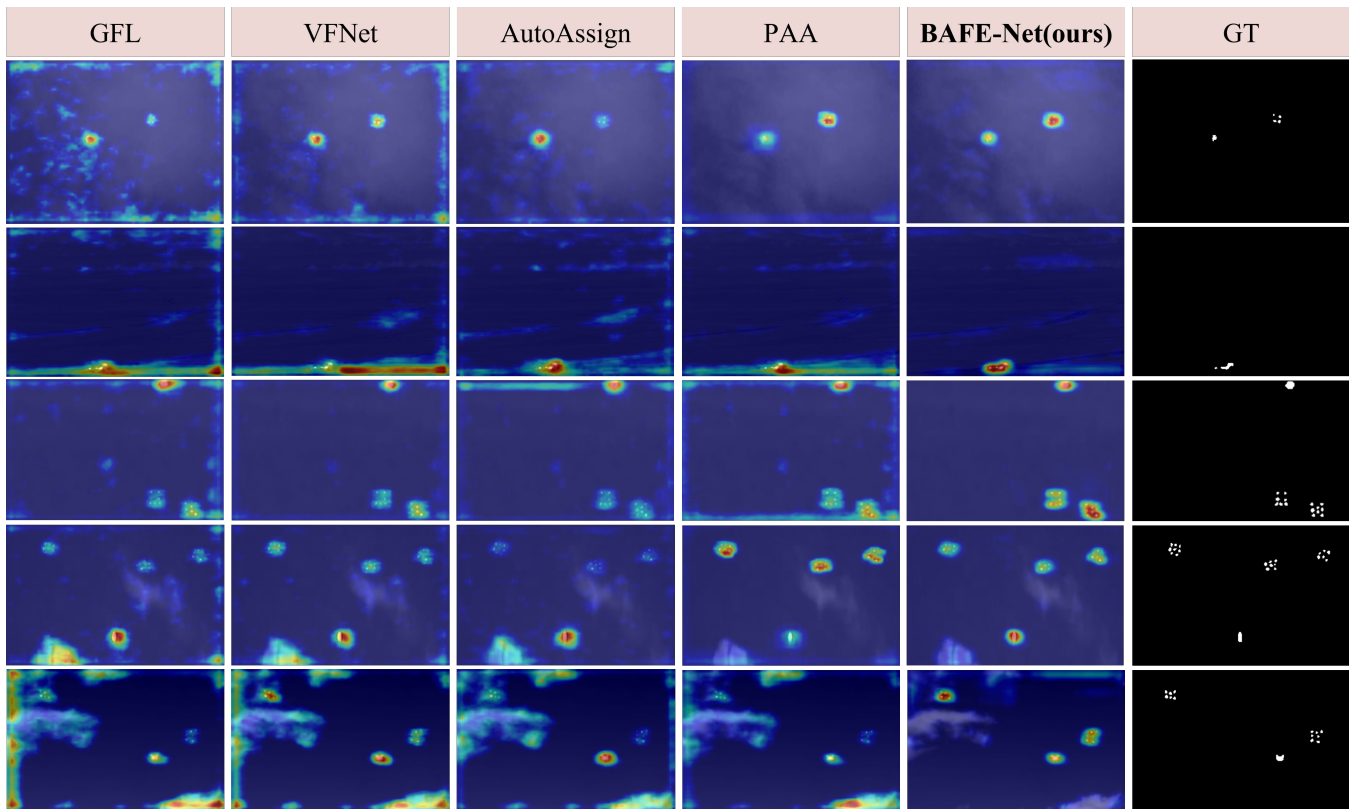


Fig. 7. Feature visualization comparison. Compared with other methods, the proposed BAFE-Net shows superior performance with higher detection of small objects and fewer false alarms.

- transactions on geoscience and remote sensing*, vol. 52, no. 1, pp. 574–581, 2013. 1, 3
- [8] Z. Qiu, Y. Ma, F. Fan, J. Huang, and L. Wu, “Global sparsity-weighted local contrast measure for infrared small target detection,” *IEEE Geoscience and Remote Sensing Letters*, vol. 19, pp. 1–5, 2022. 1
- [9] X. Wu, D. Hong, and J. Chanussot, “Uiu-net: U-net in u-net for infrared small object detection,” *IEEE Transactions on Image Processing*, vol. 32, pp. 364–376, 2022. 1
- [10] T. Wu, B. Li, Y. Luo, Y. Wang, C. Xiao, T. Liu, J. Yang, W. An, and Y. Guo, “Mtu-net: Multilevel transunet for space-based infrared tiny ship detection,” *IEEE Transactions on Geoscience and Remote Sensing*, vol. 61, pp. 1–15, 2023.
- [11] Y. Zhu, Y. Ma, F. Fan, J. Huang, K. Wu, and G. Wang, “Towards accurate infrared small target detection via edge-aware gated transformer,” *IEEE Journal of Selected Topics in Applied Earth Observations and Remote Sensing*, 2024. 3
- [12] M. Zhang, R. Zhang, Y. Yang, H. Bai, J. Zhang, and J. Guo, “Isnet: Shape matters for infrared small target detection,” in *Proceedings of the IEEE/CVF Conference on Computer Vision and Pattern Recognition, 2022*, pp. 877–886. 1, 2, 4, 5, 6
- [13] C. Feng, Y. Zhong, Y. Gao, M. R. Scott, and W. Huang, “Tood: Task-aligned one-stage object detection,” in *2021 IEEE/CVF International Conference on Computer Vision (ICCV)*. IEEE Computer Society, 2021, pp. 3490–3499. 1, 12
- [14] J. Wang, Y. Chen, Z. Zheng, X. Li, M.-M. Cheng, and Q. Hou, “Crosskd: Cross-head knowledge distillation for dense object detection,” 2023. 1
- [15] Y. Dai, Y. Wu, F. Zhou, and K. Barnard, “Asymmetric contextual modulation for infrared small target detection,” in *Proceedings of the IEEE/CVF Winter Conference on Applications of Computer Vision*, 2021, pp. 950–959. 2, 3, 5, 6
- [16] B. Li, C. Xiao, L. Wang, Y. Wang, Z. Lin, M. Li, W. An, and Y. Guo, “Dense nested attention network for infrared small target detection,” *IEEE Transactions on Image Processing*, 2022. 2, 3
- [17] X. Bai and F. Zhou, “Analysis of new top-hat transformation and the application for infrared dim small target detection,” *Pattern Recognition*, vol. 43, no. 6, pp. 2145–2156, 2010. 3
- [18] S. D. Deshpande, M. H. Er, R. Venkateswarlu, and P. Chan, “Max-mean and max-median filters for detection of small targets,” in *Signal and Data Processing of Small Targets 1999*, vol. 3809. SPIE, 1999, pp. 74–83. 3
- [19] Y. Wei, X. You, and H. Li, “Multiscale patch-based contrast measure for small infrared target detection,” *Pattern Recognition*, vol. 58, pp. 216–226, 2016. 3
- [20] L. Zhang and Z. Peng, “Infrared small target detection based on partial sum of the tensor nuclear norm,” *Remote Sensing*, vol. 11, no. 4, p. 382, 2019. 3
- [21] S. Yun, D. Han, S. J. Oh, S. Chun, J. Choe, and

- Y. Yoo, “Cutmix: Regularization strategy to train strong classifiers with localizable features,” in *Proceedings of the IEEE/CVF International Conference on Computer Vision (ICCV)*, October 2019. 4
- [22] T. DeVries and G. W. Taylor, “Improved regularization of convolutional neural networks with cutout,” *arXiv preprint arXiv:1708.04552*, 2017. 4
- [23] D. Walawalkar, Z. Shen, Z. Liu, and M. Savvides, “Attentive cutmix: An enhanced data augmentation approach for deep learning based image classification,” *arXiv preprint arXiv:2003.13048*, 2020. 4
- [24] S. Huang, X. Wang, and D. Tao, “Snapmix: Semantically proportional mixing for augmenting fine-grained data,” in *Proceedings of the AAAI Conference on Artificial Intelligence*, vol. 35, no. 2, 2021, pp. 1628–1636. 4
- [25] A. Uddin, M. Monira, W. Shin, T. Chung, S.-H. Bae *et al.*, “Saliencymix: A saliency guided data augmentation strategy for better regularization,” *arXiv preprint arXiv:2006.01791*, 2020. 4
- [26] J.-N. Chen, S. Sun, J. He, P. H. Torr, A. Yuille, and S. Bai, “Transmix: Attend to mix for vision transformers,” in *Proceedings of the IEEE/CVF Conference on Computer Vision and Pattern Recognition*, 2022, pp. 12 135–12 144. 4
- [27] M. Hong, J. Choi, and G. Kim, “Stylemix: Separating content and style for enhanced data augmentation,” in *Proceedings of the IEEE/CVF conference on computer vision and pattern recognition*, 2021, pp. 14 862–14 870. 4
- [28] J.-H. Kim, W. Choo, and H. O. Song, “Puzzle mix: Exploiting saliency and local statistics for optimal mixup,” in *International Conference on Machine Learning*. PMLR, 2020, pp. 5275–5285. 4
- [29] T. Takikawa, D. Acuna, V. Jampani, and S. Fidler, “Gated-scnn: Gated shape cnns for semantic segmentation,” in *Proceedings of the IEEE/CVF international conference on computer vision*, 2019, pp. 5229–5238. 4
- [30] I. Misra, A. Shrivastava, A. Gupta, and M. Hebert, “Cross-stitch networks for multi-task learning,” in *Proceedings of the IEEE conference on computer vision and pattern recognition*, 2016, pp. 3994–4003. 4
- [31] D. Xu, W. Ouyang, X. Wang, and N. Sebe, “Pad-net: Multi-tasks guided prediction-and-distillation network for simultaneous depth estimation and scene parsing,” in *2018 IEEE/CVF Conference on Computer Vision and Pattern Recognition (CVPR)*, 2018, pp. 675–684. 4
- [32] S. Vandenhende, S. Georgoulis, and L. Van Gool, “Mtnet: Multi-scale task interaction networks for multi-task learning,” in *Computer Vision – ECCV 2020*, 2020, pp. 527–543. 4
- [33] T. Zhang, L. Li, S. Cao, T. Pu, and Z. Peng, “Attention-guided pyramid context networks for detecting infrared small target under complex background,” *IEEE Transactions on Aerospace and Electronic Systems*, 2023. 5, 6
- [34] Z. Tian, C. Shen, H. Chen, and T. He, “Fcos: Fully convolutional one-stage object detection,” in *2019 IEEE/CVF International Conference on Computer Vision (ICCV)*, 2019, pp. 9626–9635. 7, 12
- [35] S. Fang, K. Li, and Z. Li, “Changer: Feature interaction is what you need for change detection,” *IEEE Transactions on Geoscience and Remote Sensing*, 2023. 9
- [36] W. Liu, D. Anguelov, D. Erhan, C. Szegedy, S. Reed, C.-Y. Fu, and A. C. Berg, “Ssd: Single shot multibox detector,” in *Computer Vision–ECCV 2016: 14th European Conference, Amsterdam, The Netherlands, October 11–14, 2016, Proceedings, Part I 14*. Springer, 2016, pp. 21–37. 12
- [37] X. Li, W. Wang, L. Wu, S. Chen, X. Hu, J. Li, J. Tang, and J. Yang, “Generalized focal loss: Learning qualified and distributed bounding boxes for dense object detection,” *Advances in Neural Information Processing Systems*, vol. 33, pp. 21 002–21 012, 2020. 12
- [38] S. Zhang, C. Chi, Y. Yao, Z. Lei, and S. Z. Li, “Bridging the gap between anchor-based and anchor-free detection via adaptive training sample selection,” in *Proceedings of the IEEE/CVF conference on computer vision and pattern recognition*, 2020, pp. 9759–9768. 12
- [39] X. Zhou, D. Wang, and P. Krähenbühl, “Objects as points,” *arXiv preprint arXiv:1904.07850*, 2019. 12
- [40] K. Kim and H. S. Lee, “Probabilistic anchor assignment with iou prediction for object detection,” in *Computer Vision–ECCV 2020: 16th European Conference, Glasgow, UK, August 23–28, 2020, Proceedings, Part XXV 16*. Springer, 2020, pp. 355–371. 12
- [41] W. Wang, E. Xie, X. Li, D.-P. Fan, K. Song, D. Liang, T. Lu, P. Luo, and L. Shao, “Pyramid vision transformer: A versatile backbone for dense prediction without convolutions,” in *Proceedings of the IEEE/CVF international conference on computer vision*, 2021, pp. 568–578. 12
- [42] T.-Y. Lin, P. Goyal, R. Girshick, K. He, and P. Dollár, “Focal loss for dense object detection,” in *Proceedings of the IEEE international conference on computer vision*, 2017, pp. 2980–2988. 12
- [43] M. Tan, R. Pang, and Q. V. Le, “Efficientdet: Scalable and efficient object detection,” in *Proceedings of the IEEE/CVF conference on computer vision and pattern recognition*, 2020, pp. 10 781–10 790. 12
- [44] H. Zhang, Y. Wang, F. Dayoub, and N. Sunderhauf, “Varifocalnet: An iou-aware dense object detector,” in *Proceedings of the IEEE/CVF conference on computer vision and pattern recognition*, 2021, pp. 8514–8523. 12
- [45] Q. Chen, Y. Wang, T. Yang, X. Zhang, J. Cheng, and J. Sun, “You only look one-level feature,” in *Proceedings of the IEEE/CVF conference on computer vision and pattern recognition*, 2021, pp. 13 039–13 048. 12
- [46] B. Zhu, J. Wang, Z. Jiang, F. Zong, S. Liu, Z. Li, and J. Sun, “Autoassign: Differentiable label assignment for dense object detection,” *arXiv preprint arXiv:2007.03496*, 2020. 12
- [47] X. Dai, Y. Chen, B. Xiao, D. Chen, M. Liu, L. Yuan, and L. Zhang, “Dynamic head: Unifying object detection heads with attentions,” in *Proceedings of the IEEE/CVF conference on computer vision and pattern recognition*, 2021, pp. 7373–7382. 12
- [48] S. Ren, K. He, R. Girshick, and J. Sun, “Faster r-cnn:

- Towards real-time object detection with region proposal networks,” *Advances in neural information processing systems*, vol. 28, 2015. 12
- [49] Z. Cai and N. Vasconcelos, “Cascade r-cnn: High quality object detection and instance segmentation,” *IEEE transactions on pattern analysis and machine intelligence*, vol. 43, no. 5, pp. 1483–1498, 2019. 12
- [50] H. Zhang, H. Chang, B. Ma, N. Wang, and X. Chen, “Dynamic r-cnn: Towards high quality object detection via dynamic training,” in *Computer Vision–ECCV 2020: 16th European Conference, Glasgow, UK, August 23–28, 2020, Proceedings, Part XV 16*. Springer, 2020, pp. 260–275. 12
- [51] X. Lu, B. Li, Y. Yue, Q. Li, and J. Yan, “Grid r-cnn,” in *Proceedings of the IEEE/CVF conference on computer vision and pattern recognition*, 2019, pp. 7363–7372. 12
- [52] J. Pang, K. Chen, J. Shi, H. Feng, W. Ouyang, and D. Lin, “Libra r-cnn: Towards balanced learning for object detection,” in *Proceedings of the IEEE/CVF conference on computer vision and pattern recognition*, 2019, pp. 821–830. 12
- [53] N. Carion, F. Massa, G. Synnaeve, N. Usunier, A. Kirillov, and S. Zagoruyko, “End-to-end object detection with transformers,” in *Computer Vision–ECCV 2020: 16th European Conference, Glasgow, UK, August 23–28, 2020, Proceedings, Part I 16*. Springer, 2020, pp. 213–229. 12
- [54] X. Zhu, W. Su, L. Lu, B. Li, X. Wang, and J. Dai, “Deformable detr: Deformable transformers for end-to-end object detection,” *arXiv preprint arXiv:2010.04159*, 2020. 12
- [55] S. Liu, F. Li, H. Zhang, X. Yang, X. Qi, H. Su, J. Zhu, and L. Zhang, “Dab-detr: Dynamic anchor boxes are better queries for detr,” *arXiv preprint arXiv:2201.12329*, 2022. 12
- [56] D. Meng, X. Chen, Z. Fan, G. Zeng, H. Li, Y. Yuan, L. Sun, and J. Wang, “Conditional detr for fast training convergence,” in *Proceedings of the IEEE/CVF international conference on computer vision*, 2021, pp. 3651–3660. 12
- [57] P. Sun, R. Zhang, Y. Jiang, T. Kong, C. Xu, W. Zhan, M. Tomizuka, L. Li, Z. Yuan, C. Wang *et al.*, “Sparse r-cnn: End-to-end object detection with learnable proposals,” in *Proceedings of the IEEE/CVF conference on computer vision and pattern recognition*, 2021, pp. 14 454–14 463. 12